6th International Symposium on Three-Dimensional Electromagnetics
Berkeley, California, March 28–30, 2017

3D individual and joint inversion of DC resistivity and EM data

J. Weißflog[1], F. Eckhofer[2], R.-U. Börner[1], M. Eiermann[2], O.G. Ernst[3], and K. Spitzer[1]
[1] Institute of Geophysics and Geoinformatics, TU Bergakademie Freiberg
[2] Institute of Numerical Mathematics and Optimization, TU Bergakademie Freiberg
[3] Department of Mathematics, TU Chemnitz

Summary

The aim of our project is the combination of different electromagnetic and DC resistivity methods in a joint inversion to enhance the overall resolution power. Every method is associated with a particular sensitivity pattern and therefore appropriate to explore different regions of the subsurface. By combining complementary patterns, electromagnetic imaging becomes more complete and reliable. The enhanced coverage helps to reduce the problem of noisy data and measurement errors and improves the reconstruction of the given conductivity distribution. All forward operators are formulated using finite elements on unstructured grids. We suggest a sequential inversion strategy that cycles through the different EM methods iteratively instead of setting up one big system of equations. To link the methods together we make use of a regularization operator that penalizes the deviation of the model parameters from the inversion result of the previous method. Thus, we do not have to determine the full set of regularization parameters at once which is a major difficulty due to their inherent uncertainty. In a first step, we show that this approach can be successfully applied to synthetic models and that the combination of two methods yields a significantly improved resolution compared to the individual DC or EM inversion. Future work will incorporate an appropriate suite of EM methods adopted to the requirements of a specific exploration task.

Keywords: joint inversion, DC resistivity method, electromagnetic method, smoothness regularization

Introduction

As a part of the ongoing research and advancement of available methods, we developed two new modeling and inversion codes for dealing with DC resistivity and electromagnetic data. The codes are partially based on known algorithms, but we also examined and implemented new approaches. Each of the two individual codes enables us to simulate and invert the particular data sets. All parts of the software are implemented in MATLAB to achieve standardization of our codes and establish a flexible and state-of-the-art software basis to simplify the work with more than one geophysical method.

The new DC resistivity and electromagnetic forward operators are using finite elements on unstructured tetrahedral grids that can easily be combined with our already existing TEM software (Afanasjew et al., 2010) and others. This code enables us to deal with even complex topography and to extract the derivatives, which are crucial for the inversion while retaining full control over the assembly process of the system matrix (Weißflog et al., 2012).

For simplicity, we apply a regularized Gauss-Newton method in view of a combination of different electromagnetic methods in one inversion algorithm. We focus on an appropriate regularization technique that has been outlined by Schwarzbach and Haber (2012). Finally, we present a sequential approach to joint inversion, where we combine both codes to improve the inversion result. This sequential approach overcomes several difficulties concerning data weighting and a regularization for more than one geophysical method.

Smoothness Regularization

The inversion process requires us to solve a minimization problem which combines the residual norm and a regularization functional:

$$\Phi(\boldsymbol{m}) = \|Q\boldsymbol{u} - \boldsymbol{b}\|_2^2 + \beta R(\boldsymbol{m} - \boldsymbol{m}_{\text{ref}}) \to \min_{\boldsymbol{m}} \quad (1)$$

subject to $A(\boldsymbol{m})\boldsymbol{u} = \boldsymbol{f}$. Here, $\boldsymbol{b}$ is the measured data, $\boldsymbol{u} = A(\boldsymbol{m})^{-1}\boldsymbol{f}$ the modeled data, $\boldsymbol{m}$ are the model parameters, Q is some measurement operator ($Q\boldsymbol{u} \approx \boldsymbol{b}$), $\boldsymbol{m}_{\text{ref}}$ is the reference model and β represents the regularization parameter.

To stabilize the inversion procedure and provide additional information to avoid ambiguities, a suitable regularization strategy is necessary. As our inversion approach is based on a finite element discretization using a piecewise constant representation of the conductivity model, this requires a regularization operator applicable to piecewise constant model parameters on unstructured grids and weak formulations.

We have implemented a smoothness regularization in which the penalty function measures the norm of a weak gradient of the conductivity field:

$$R(m) = \tfrac{1}{2} \int_\Omega |\nabla(m - m_{\text{ref}})|^2 \, dV,$$

with $m \in H^1(\Omega)$. Because the parameters m are not differentiable across element boundaries, we derive a generalized (mixed) formulation of the regularization operator as laid out in Brezzi and Fortin (1991):

$$\Phi^{\text{Reg}}(m, \boldsymbol{p}) = -\beta \left(\tfrac{1}{2} \int_\Omega |\boldsymbol{p}|^2 \, dV + \int_\Omega (m - m_{\text{ref}}) \nabla \cdot \boldsymbol{p} \, dV \right), \quad (2)$$

with $m \in L^2(\Omega)$ and $\boldsymbol{p} \in H_0(\text{div}; \Omega) = \{\boldsymbol{p} \in L^2(\Omega)^3; \nabla \cdot \boldsymbol{p} \in L^2(\Omega); \boldsymbol{n} \cdot \boldsymbol{p}|_{\partial\Omega} = 0\}$.

To achieve a conforming discretization we use Raviart-Thomas elements of lowest order (RT_0). This ensures continuity of normal components across elements. We are able to eliminate the dual variable $\boldsymbol{p}$ and the discrete representation of (2) then reads:

$$\Phi^{\text{Reg}}(\boldsymbol{m}) = \tfrac{\beta}{2} (\boldsymbol{m} - \boldsymbol{m}_{\text{ref}})^T D M^{-1} D^T (\boldsymbol{m} - \boldsymbol{m}_{\text{ref}}),$$

with the RT_0 mass matrix M and the discrete divergence operator D.

Applying a Gauss-Newton scheme to solve the nonlinear least squares problem enables us to linearize $\Phi(\boldsymbol{m})$. The resulting linear problem is solved by an iterative Krylov subspace method to find a better approximation to the model parameters $\boldsymbol{m}$ in each Gauss-Newton step.

A sequential approach to joint inversion

The interpretation and inversion of geophysical data has been investigated for many decades and even the combined or joint inversion of different geophysical methods is not new, but there are significant differences in each scheme. In general, the term *joint inversion* stands for the combination of two or more different geophysical methods and sometimes different petrophysical parameters in one inversion approach to enhance the overall resolution power. Using joint inversion we can overcome some of the ambiguities and uncertainties which are intrinsic in each of the individual methods (Sasaki (1989), Raiche, Jupp, Rutter, and Vozoff (1985), Haber and Oldenburg (1997)). Each method is sensitive to a certain depth and parameter range and yields distinct parameter models of the Earth (Albouy et al., 2001).

There are several possibilities to implement a combined inversion using different data sets. Most of the literature, e.g. Meju (1996) or Commer and Newman (2009), talk about a joint inversion where the minimization problem given in equation (1) is extended by adding a data residual norm for each additional geophysical method.

We present a sequential approach to joint inversion as follows: The data set of the first method is inverted separately with its own regularization strategy and for example a homogeneous reference model equal to the background conductivity. Then, we use the final result of the first method ($\boldsymbol{m}_1$) as reference model for the second method. The objective function for the minimization problem of the second geophysical method reads as follows:

$$\begin{aligned} \Phi_2(\boldsymbol{m}) &= \tfrac{1}{2} \|Q\boldsymbol{u} - \boldsymbol{b}\|_2^2 + \tfrac{\beta}{2} ||W(\boldsymbol{m} - \boldsymbol{m}_{\text{ref}})||^2 \\ &= \tfrac{1}{2} \|Q\boldsymbol{u} - \boldsymbol{b}\|_2^2 + \tfrac{\beta}{2} ||W(\boldsymbol{m} - \boldsymbol{m}_1)||^2. \end{aligned}$$

The result of the second inversion includes information of both methods and can now be used as input for a third inversion and so on.

Because we implement a separate inversion for each geophysical method, we do not have to think about weighting the different data sets against each other. Just a weighting within one data set concerning for example depth of resolution can be useful. Furthermore, we have to find a suitable regularization strategy and parameter for only one method and do not have to include all data sets in one parameter regularization. The reference model is free for the first inversion where we usually use a homogeneous or layered background. In all following calculations we use the one we get as result of the previous inversion scheme. Another big advantage is the independence from the programming language. It is possible to implement all the methods in a different language and just hand the final parameter vector over to another code. People from different working groups might work together more easily in this approach. The only intersection we have to think about is the inversion mesh which is the distribution of model parameters. This should be the same for all methods. Otherwise, we have to do a difficult interpolation of data which will worsen the inversion's result.

In the numerical experiments, we combine 3D DC resistivity and VLF-R data to improve the inversion result. We apply our joint inversion approach to the downscaled 3D-2 COMMEMI model (Zhdanov, Varentsov, Weaver, Golubev, & Krylov, 1997) with a vertical extent of 100 m.

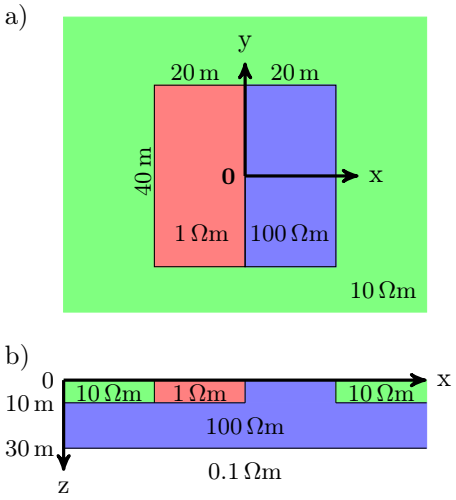

Figure 1: Plan view (a) and slice (b) of the 3D-2 COMMEMI model.

It was discretized into a relatively coarse mesh consisting of 2241 parameters. Figure 2a shows a plan view of the true model consisting of one conductive and one resistive block compared to the 0.1 $\frac{\mathrm{S}}{\mathrm{m}}$ background. The objective functions for both methods are given as follows:

$$\Phi(\boldsymbol{m}_{\mathrm{dc}}) = \|Q_1\boldsymbol{u}_1 - \boldsymbol{b}_1\|_2^2 + \tfrac{\beta_1}{2}\|W_1(\boldsymbol{m}_{\mathrm{dc}} - \boldsymbol{m}_{\mathrm{ref}})\|_2^2$$
$$\Phi(\boldsymbol{m}_{\mathrm{vlf}}) = \|Q_2\boldsymbol{u}_2 - \boldsymbol{b}_2\|_2^2 + \tfrac{\beta_2}{2}\|W_2(\boldsymbol{m}_{\mathrm{vlf}} - \boldsymbol{m}_{\mathrm{ref}})\|_2^2.$$

The individual inversion for the DC resistivity method was carried out using nine equidistant sources between $x/y = -30$ m and $x/y = 30$ m at the Earth's surface (Figure 2c, black dots) and 49 receivers inside the source configuration producing 441 apparent resistivity data points. We added three percent random noise. We use a homogeneous starting model of 0.1 $\frac{\mathrm{S}}{\mathrm{m}}$ and the layered background as reference model within our smoothness regularization. To find an optimal starting value for the regularization parameter β we use the ratio of the data residual and regularization norm. According to our problem definition, we set $\beta_1 = 2.33$. To give more weight to the data residual with progressing inversion we decreased β by a factor of 10 in each Gauss-Newton step until it reached a value of 10^{-3}. A simple damping algorithm is applied. Figure 2c shows the individual DC resistivity result. Surface charges force the electric current to concentrate in a conductive body which yields a much better reconstruction of the conductive block compared to the resistive one.
For the VLF-R method, we used a transmitter frequency of 20 kHz and measured the components E_x and H_y at 50 receiver locations on a single profile at the Earth's surface ($z = y = 0$ m) between $x = -70$ m and $x = 70$ m. The synthetic data set includes three percent random noise as well. We use a resistive homogeneous starting model of 0.01 $\frac{\mathrm{S}}{\mathrm{m}}$ and again the layered reference model. The regularization parameter β was decreased by a factor of 10 in each step from 10^2 to 10^{-5}. In Figure 2b we see the individual VLF-R result. Due to the skin effect which describes the decay behavior of the electromagnetic field, the resolution of the resistive block is a bit better than for the conductive block. Understandably, with one profile in the center of the model, we are not able to get the exact boundaries of the embedded blocks. Data from the perpendicular polarization will improve this result.

The joint optimization problem is given as follows: Find the model parameters $\boldsymbol{m}_{\mathrm{dc}}$ such that

$$\Phi(\boldsymbol{m}_{\mathrm{dc}}) = \|Q_1\boldsymbol{u}_1 - \boldsymbol{b}_1\|_2^2 + \tfrac{\beta_1}{2}\|W_1(\boldsymbol{m}_{\mathrm{dc}} - \boldsymbol{m}_{\mathrm{ref}})\|_2^2$$
$$= \|Q_1\boldsymbol{u}_1 - \boldsymbol{b}_1\|_2^2 + \tfrac{\beta_1}{2}\|W_1(\boldsymbol{m}_{\mathrm{dc}} - \boldsymbol{m}_{\mathrm{vlf}})\|_2^2$$

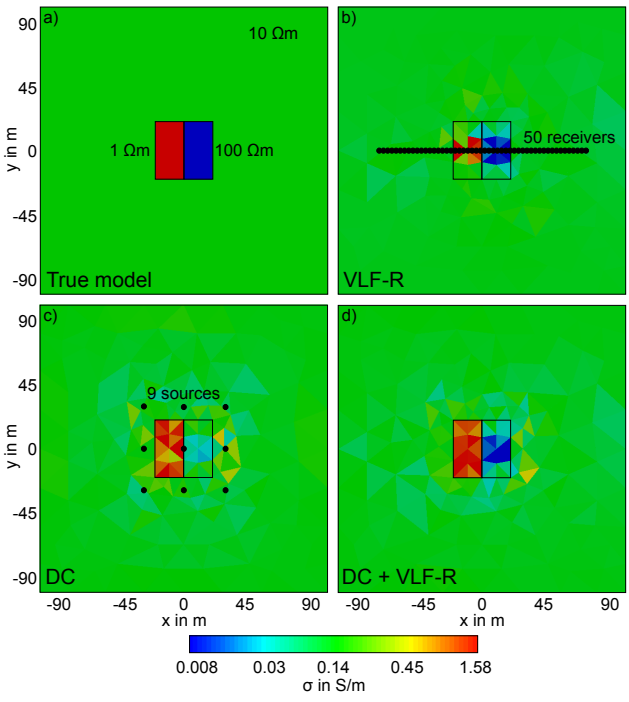

Figure 2: Plan view of the downscaled 3D-2 COMMEMI model. a) The true model used to compute the synthetic data. b) and c) are the inversion results for the individual VLF-R and DC resistivity inversion, respectively. d) Using the DC resistivity solution as the reference model, we then inverted the VLF-R data to obtain a joint inversion result, which recovers the two anomalous bodies well.

is minimized. As described in the previous section, we use the result of one method as reference model for the second method to exploit the different sensitivity patterns. Here, we use the inverted VLF result as input for the DC inversion. We give a bit more weight to the regularization norm and set the lower limit for β to be 10^{-2} in order to keep the result close to the VLF model. All other parameters stay the same as for the individual DC inversion. The iteration was terminated after 20 Gauss-Newton steps with a relative residual norm of $4.1{\cdot}10^{-2}$. The overall resolution of the joint result in Figure 2d is better than the simple addition of both individual results. We clearly see an improved image of the conductive block compared to the DC resistivity inversion as well as small improvements in the resistive block. Using the final result again as input for one of the individual inversions does not change the resulting conductivity model. It is also possible to run the sequential joint inversion the other way round: Using the DC result as reference model for the VLF inversion. Because there is no improvement in the final conductivity model, we leave this result out. A further sequential iteration also yields no improvement.

REFERENCES

Afanasjew, M., Börner, R.-U., Eiermann, M., Ernst, O., Güttel, S., & Spitzer, K. (2010, Sep 18 – 24, 2010, Giza, Egypt). 2D Time Domain TEM Simulation Using Finite Elements, an Exact Boundary Condition, and Krylov Subspace Methods, Extended Abstract. *Proceedings:* 20^{th} *International Workshop on Electromagnetic Induction in the Earth*, 4p.

Albouy, Y., Andrieux, P., Rakotondrasoa, G., Ritz, M., Descloitres, M., Join, J.-L., & Rasolomanana, E. (2001). Mapping coastal aquifers by joint inversion of dc and tem soundings-three case histories. *Ground Water*, *39*(1), 87–97.

Brezzi, F., & Fortin, M. (1991). *Mixed and hybrid finite elements methods.* Springer-Verlag.

Commer, M., & Newman, G. A. (2009). Three-dimensional controlled-source electromagnetic and magnetotelluric joint inversion. *Geophysical Journal International*, *178*(3), 1305–1316.

Haber, E., & Oldenburg, D. W. (1997). Joint inversion: a structural approach. *Inverse Problems*, *13*(1), 63-77.

Meju, M. A. (1996). Joint inversion of tem and distorted mt soundings; some effective practical considerations. *Geophysics*, *61*(1), 56-65.

Raiche, A. P., Jupp, D. L. B., Rutter, H., & Vozoff, K. (1985). The joint use of coincident loop transient electromagnetic and schlumberger sounding to resolve layered structures. *Geophysics*, *50*(10), 1618-1627.

Sasaki, Y. (1989). Two-dimensional joint inversion of magnetotelluric and dipole-dipole resistivity data. *Geophysics*, *54*(2), 254-262.

Schwarzbach, C., & Haber, E. (2012). Finite element based inversion for time-harmonic electromagnetic problems. *submitted to Geophysical Journal International*.

Weißflog, J., Eckhofer, F., Börner, R.-U., Eiermann, M., Ernst, O., & Spitzer, K. (2012, Aug 25 – 31, 2012, Darwin, Australia). 3D DC resistivity FE modelling and inversion in view of a parallelised Multi-EM inversion approach, Extended Abstract. *Proceedings:* 21^{st} *Electromagnetic Induction Workshop*, 4p.

Zhdanov, M. S., Varentsov, I. M., Weaver, J. T., Golubev, N. G., & Krylov, V. A. (1997). Methods for modelling electromagnetic fields results from commemi—the international project on the comparison of modelling methods for electromagnetic induction. *Journal of Applied Geophysics*, *37*(3–4), 133 - 271. (Methods for modelling electromagnetic fields)